Determining the peritectic transition time under continuous casting conditions of hyper-peritectic steels

B. Santillana[1], B. G. Thomas[2], D.W. van der Plas[1], D. Ruvalcaba [1], A.J.C. Burghardt[1]

1 Tata Steel, Research & Development, The Netherlands
2 University of Illinois at Urbana-Champaign, USA

E-mail: begona.santillana@tatasteel.com

Abstract. During continuous casting, local solidification kinetics influences the phase transitions in steels. The rate and temperature at which the transitions occur determines in part the mechanical behaviour of the solidifying steel. Severe tension may occur during the peritectic transition due to the local shrinkage which accompanies the transformation from Ferrite to Austenite. This may lead to internal or surface crack formation. The susceptibility to crack formation, and location of the cracks, are related to both the solid-state phase transitions and the solid fraction within the mushy (semi-solid) region. Casting parameters, such as casting speed, heat flux, and fluid flow among others, influence the local solidification kinetics (i.e. the rate at which the transition from liquid to solid occurs). A proper balance of the important parameters may reduce crack formation and propagation, by adjusting the peritectic transition towards a less crack sensitive region within the mush. The present study investigates the influence of casting speed on the local peritectic transition time during the solidification of a hyper-peritectic steel. The peritectic transition has been determined in two steps: first, the CON1D model was used to determined the influence of casting speed on the local cooling rate within the solidified shell close to mould exit; second, the cooling rate is used as boundary condition in DICTRA in order to determine the local peritectic transition time.

1. Introduction

The continuous casting process requires careful selection of process parameters (such as casting speed, superheat, etc.) which determine the castability (i.e. the degree of ease in casting an alloy for producing a good quality cast product) of a given grade of steel slabs. It is important to understand the influence of these casting parameters on slab operation and steel quality in order to provide the best casting practices in the plant. Furthermore, the best casting practice can facilitate the processing of slabs downstream by having uniform slabs with good mechanical properties.

The solidification process determines the chemical homogeneity, dendrite structure and mechanical properties of the solid skin. This solidifying shell must be sufficiently thick, strong and uniform to maintain geometric stability while sustaining stresses from internal pressure, mechanical and thermal loads. Moreover, the stability of the solidifying skin is determined by the thermo-physical properties of the steel alloy. These properties are determined by the steel composition.

Multicomponent steels present several castability challenges due to their inherent thermo-physical properties and transition of phases during solidification. Phase transitions and the formation of secondary phases during solidification, such as precipitates, may lead to local stress variations which

can cause the nucleation of cracks within the mush (i.e. semi-solid dendritic network). Peritectic steels are susceptible to crack formation during solidification due to the formation of γ-austenite from the liquid L and δ-ferrite phases which is accompanied by local volumetric shrinkage upon cooling. This peritectic transition: L+ δ + γ → γ has been widely studied and found to be critical in determining the castability of multicomponent steels [1-8]. This has been attributed to uneven shell growth caused by the large volume contraction during the peritectic transition that makes the solidified shell detach locally from the mould wall. Local contraction can contribute to the formation of weak spots that may lead to thinner solid skin caused by the lack of heat release towards the mould wall. When stress is applied to the shell, these thin and weak regions may tear and crack [8]. An important factor to indicate crack propagation and failure is the proximity of the solidus point to the peritectic transition. Figure 1 shows the influence of C content on the transition of phases as presented in the Fe-C phase diagram. This diagram illustrates a suggested origin of surface problems due to the type of phase transitions related to C content, where in the transition L + δ to δ + γ the steel is susceptible to depressions due to shrinkage associated to the δ to γ phase transition [9].

The duration of the peritectic transition greatly affects crack susceptibility. Solid-state phase transitions close to the solidus temperature may cause cracking [1, 3, 4, 6, 8, 9]. This is usually above a fraction of solid of f_S~ 0.85. On the other hand, cracks that develop at low fractions of solid may be healed with liquid. The healing of a crack by liquid flow will depend on the permeability of the mush which in turn depends on the dendritic structure.

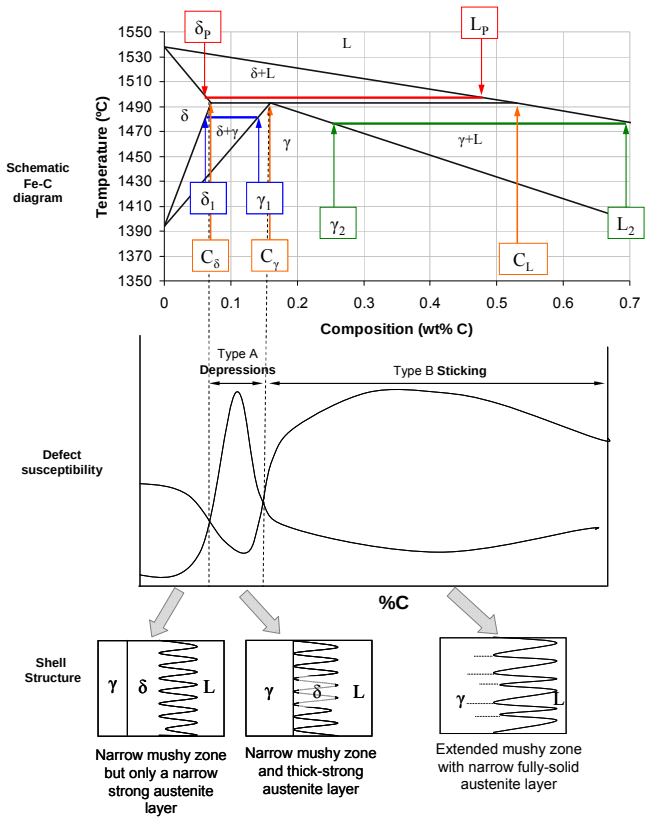

Figure 1. A suggested origin of the 'Peritectic' surface quality problems [10, 11]

Nowadays, the commercial steel grades are far more complex than the "typical Fe-C grades", where a simple pragmatic approach has been to translate the effect of the other alloying elements to the effect on a Fe-C pseudo-binary phase diagram.

Changes in the Fe–C phase diagram from other alloying elements can be described using an effective carbon content Cp. This "carbon equivalent" approach has been widely used as an empirical approximation to how alloying elements affect the formations of phases. In this method, γ-austenite forming elements add to the C content and δ-ferrite forming elements are subtracted. The steel grade is categorised as hypo-peritectic, peritectic or hyper-peritectic. However, this method fails to consistently predict the castability of different steel grades, as it does not account for the particular casting conditions. The influence of casting conditions on solidification kinetics (i.e. rate at which the transition from liquid to solid occurs) and phase transitions sequence is not well understood and needs further study.

Another important aspect to consider in multicomponent steels is that the addition of alloying elements leads to an enlargement of the mushy region. This effect increases the propensity to crack formation due to a wider transition region whereby stresses can vary significantly. In addition to steel composition, the mushy region is also influenced by the local cooling rate determined by the heat flux and casting speed. Therefore, an integrated modelling approach is required to understand the influence of casting parameters on solidification kinetics for improving the castability of difficult steel grades.

This paper presents an integrated modelling approach for determining the castability of hyper-peritectic steels. Considering that the peritectic transition is also governed by solute diffusion, the local peritectic transition time is determined using Thermo-Calc and DICTRA based on the local cooling conditions within the mush estimated by CON1D. This method facilitates the integration of cooling conditions determined by the actual casting conditions in a slab caster, in order to aid in assessing casting parameters to produce these steels.

2. Materials and methods

A typical hyper-peritectic steel was selected for the current study, having an aim composition of: 0.15 wt.% C, 2.0 wt.% Mn, and 0.5 wt.% Si. It is important to understand the solidification of these types of steels, since they can be crack sensitive. This may not be only due to the peritectic transition, but also due to the enlargement of the mushy region as a result of solute enrichment in the liquid (microsegregation) causing the solidus temperature to drop locally. These types of steels should have the following phase transition sequence during solidification: $L \rightarrow L + \delta \rightarrow L + \delta + \gamma \rightarrow L + \gamma \rightarrow \gamma$.

For this study, the influence of casting speed V_C on the local peritectic transition time was investigated. The casting speed is a critical parameter to be controlled during continuous casting. The castability of hyper-peritectic steels may depend greatly on this parameter. In order to perform a comparative study, we investigated three casting speeds: V_C=1.0 and 1.75 m/min, which can be reached in conventional slab caster; and a V_C= 5.5 m/min, which can be reached in a thin slab caster. Then the influence of local cooling rate on the peritectic transition was investigated. It is certainly a challenge to cast hyper-peritectic steels at a high speed such as 5.5 m/min.

3. Integrated modelling approach

3.1. CON1D modelling

CON1D is a program developed by the University of Illinois which simulates the heat transfer and solidification of the steel alloy in the mould region during slab casting [12, 13]. The 1-D finite difference model estimates the local cooling and solidification based on the casting conditions determined by parameters such as heat flux, casting speed and slag layer thickness. The model also resolves the local contraction during solidification which determines the air gap formation and thus gives a better estimation of the profiles of local heat flux and solid skin formation inside the mould. Figure 2 shows the schematic representation of the model for determining the vertical lines at different depths from the mould/slab contact interface inwards. The shell vertical lines can be distributed along the shell thickness and a maximum of 10 vertical lines can be calculated. The output is displayed either per millimetre (distance below meniscus) or by using the casting speed, per second (time).

Figure 2 also shows the heat flux curve, determined by the casting conditions, which influences the local cooling rate inside the mould.
CON1D can also calculate the non-equilibrium phase fraction / temperature relation of a given plain carbon steel alloy, including the liquidus and solidus temperatures. This calculation is based on a simple microsegregation model for steel that extends the Clyne–Kurz model to account for multiple components and the peritectic transformation, as described elsewhere [14]. It considers the separate temperature-dependent diffusion and partition coefficients of 14 different elements in both the austenite and delta-ferrite phases [15].

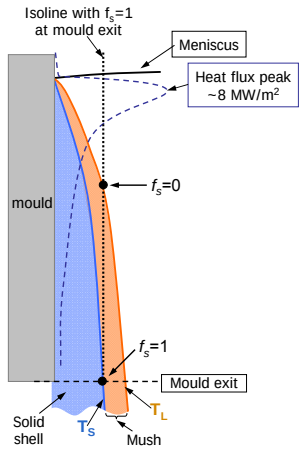

Figure 2. Schematic drawing of the position of the selected vertical lines in CON1D.

When selecting the liquidus temperature in each vertical line as the starting point for a fraction of solid f_S=0 and in the same way the solidus as the finishing point when f_S=1, it is possible to plot the cooling rate versus the fraction of solid for each vertical line as seen in Figure 3. In the current study we determine the vertical line which has the end of solidification f_S=1 close to mould exit. Since, at this region, fluctuations in solidification and local stresses can be more critical in determining the castability of these steels, the casting process can be more susceptible to local changes in solidification due to the fact that the slab is no longer being supported by the walls after leaving the mould and it is only supported by its own solidified skin.

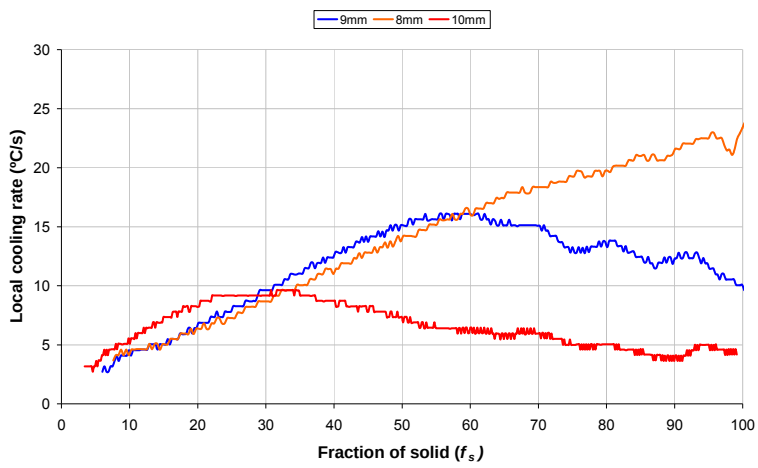

Figure 3. Calculated with CON1D local cooling rate as a function of fraction of solid for the case at 5.5 m/min of casting speed.

In order to select the appropriate vertical lines, the solid skin thickness at mould exit was determined for each case and then the vertical line chosen for studying the local solidification was selected. The chosen vertical lines were those that approximately reach a f_S=1 at mould exit. The cooling rate changes and local solidification time was then determined for the cases shown in Table 1. The curves shown in Figure 3 (as example for the V_C= 5.5 m/min) were used in DICTRA and also for estimating the local solidification time t_S. Table 1 shows the local solidification time t_S and an estimation of the average cooling rate ΔT/Δt (for comparison) based on the calculated curves for the three cases. The local cooling rates were obtained at steady-state casting conditions. The mushy zone thickness is the difference between the shell thickness with an f_S=1 and the shell with an f_S=0. The tabulated "shell thickness" is the thickness of the shell with a f_S=0.9.

Table 1. Summary of the solidification characteristics determined in CON1D for the cases studied.

Vc (m/min)	t_S (s)	ΔT/Δt (°C/s)	λ_2 (μm)	Mushy zone thickness (mm)	Shell thickness (mm)	vertical line distance (mm)
1	15	~2,5	73	6	19.35	19
1.75	11	~3,5	65	4.9	14.15	14
5.5	3	~11	42	1.8	9.5	9
*	3	~11	200	-	-	-

* hypothetical case

3.2. Thermodynamic and kinetic modelling

Themo-Calc and DICTRA were used for determining the solidification kinetics and to resolve the peritectic transition as a function of time based on the local cooling rate. The cooling rate curves as a function of fraction of solid and local solidification time, obtained from CON1D, were used to construct the DICTRA 1-D model. Since the peritectic transition is governed by solute diffusion, this approach should give a better appreciation of the influence of casting parameters on the local solidification.

The databases TCFE6 version 6.2 and MOB2 version 2.6 were used in Thermo-Calc and DICTRA [16]. The size of the 1-D domain in DICTRA was considered as the half-symmetry of the theoretical secondary dendrite arm spacing (λ_2) determined as in [17]:

$$\lambda_2 = 26.1 \times t_S^{0.38}$$

Table 1 summarizes the input for the three different cases. The λ_2 (in μm) is considered as a representative solidifying volume which moves from the liquidus towards the solidus within the mushy region during solidification.

In addition to the cases where the local cooling was determined from CON1D, an additional hypothetical case was considered. As shown in Table 1, it was set-up with the same cooling rate as the case with V_C= 5.5 m/min, i.e. ΔT/Δt~ 11 °C/s; but a larger secondary dendrite arm spacing was considered, λ_2= 200 μm. This was done to compare the influence of local solidification conditions on the peritectic transition.

4. Results and discussion

The progression on solidification upon cooling can be better visualized in Figure 4, where the calculated solidification curves from Thermo-Calc and DICTRA for the different cases studied are shown. The calculated solidification paths based on local cooling rates and λ_2 are shown in the DICTRA curves. These solidification paths are in between the two solidification extremes i.e. Equilibrium and Scheil. For this Scheil calculation, only C is assumed to back diffuse during solidification (as being an interstitial element). The solidus temperature in the Scheil approximation drops significantly as shown in Figure 4. The local cooling rate, influenced by the casting speed, can

reflect more precisely the local solidification kinetics which in turn influences the peritectic transition time in DICTRA. The DICTRA calculation has limited diffusion of elements constrained by the local solidification conditions, and thus, the solidus temperature does not drop as much as compared to the Scheil calculation.

The solidification curves in equilibrium and Scheil show a slope which indicates the temperature at which the peritectic transition occurs. In equilibrium, the peritectic transition (whereby L + δ + γ coexist) occurs at 1484 °C, having the start at f_S= 0.72 and the end at f_S=0.85. The same transition in Scheil starts at a lower temperature (1480 °C) and occurs at a lower fraction of solid, between f_S= 0.70 and f_S=0.79, as compared to equilibrium. This is due to the segregation of solute elements in the liquid at the solid/liquid interface leading to the formation of γ-austenite at a slightly lower temperature and fraction of solid. From this point onwards, the γ-austenite forms from the remaining liquid. This highlights the influence of microsegregation on the peritectic transition during solidification. The equilibrium calculation indicates that the solidification of the hyper-peritectic steel may be more susceptible to cracking as compared to the Scheil solidification. Since in the equilibrium calculation, the transition occurs at a higher f_S as compared to the Scheil solidification, whereby the transition occurs at a lower f_S. Also, the solid fraction range during the transition is wider in equilibrium, as compared to Scheil solidification, which increases the propensity to cracking.

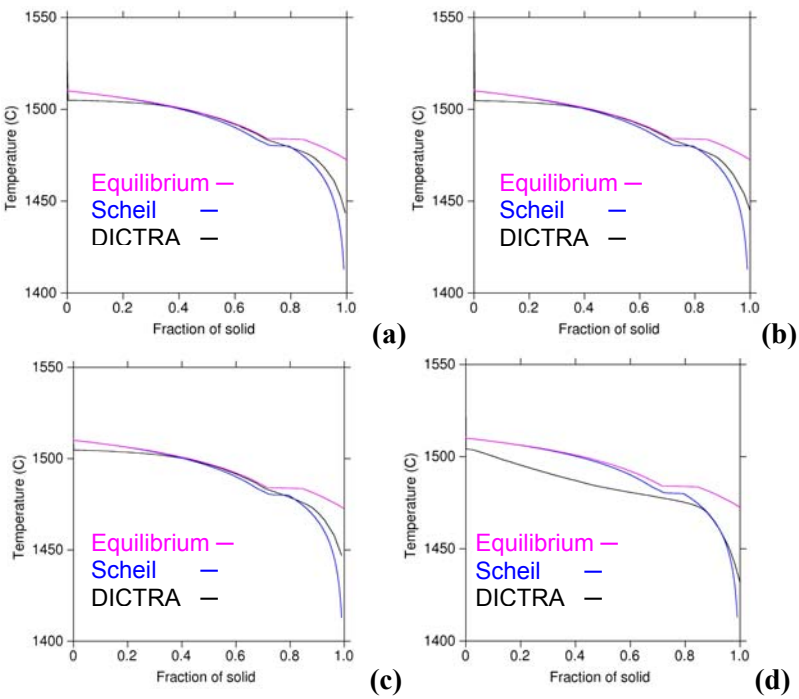

Figure 4. Solidification curves for the cases: a) V_C=1.0 m/min, b) V_C=1.75 m/min, c) V_C=5.5 m/min, and d) ΔT/Δt= 11°C/s and λ_2= 200 μm.

The solidification paths obtained from DICTRA showed no great differences based on the different casting speeds studied here. Moreover, the solidification curves do not show clearly where the transition occurs. This last characteristic in the curves is because the cooling rates used for this study are obtained from CON1D which has been validated against actual casting parameters [18]. The fact that is little difference is because the thin slab caster simulation does use other casting parameters to account for the much higher heat extraction. The estimated local cooling does not reflect the local undercooling at the start of solidification and the latent heat released due to the peritectic transformation and local solidification which can be seen in real solidification conditions. Still, the

transition can be appreciated in Figure 5, whereby the phase formation (δ and γ) can be seen as a function of the total fraction of solid f_S. It was found that the local cooling rates determined here do not show a great impact on the phase formation as a function of total fraction of solid f_S. On the other hand, the hypothetical case having a larger λ_2 (200 μm) shows a dissimilar solidification path and peritectic transition as compared to the other cases. The solidification curve moves to lower temperatures and the peritectic transition occurs at a wider range of fraction of solid, leading to a higher propensity for cracking (Figure 4d).

The DICTRA calculations showed the start of the peritectic transition at: T= 1484 °C and f_S = 0.7, and the end at: T= 1475 °C and f_S = 0.86 for the three cases considered here. The results also showed that the peritectic transition occurs over a temperature range upon cooling, as compared to the equilibrium and Scheil calculations, which showed the transition at a single temperature. The peritectic transition for these casting speeds occurs at relatively similar range of solid fraction as that at equilibrium.

The solidification curves in figure 4 show that the DICTRA calculations have a lower liquidus temperature as compared to the two solidification extremes (equilibrium and Scheil). The drop in the liquidus temperature is due to the local solute enrichment in the liquid at the solid-liquid interface. The equilibrium and Scheil calculations consider a uniform composition in the liquid phase during solidification following the liquidus line in the equilibrium phase diagram.

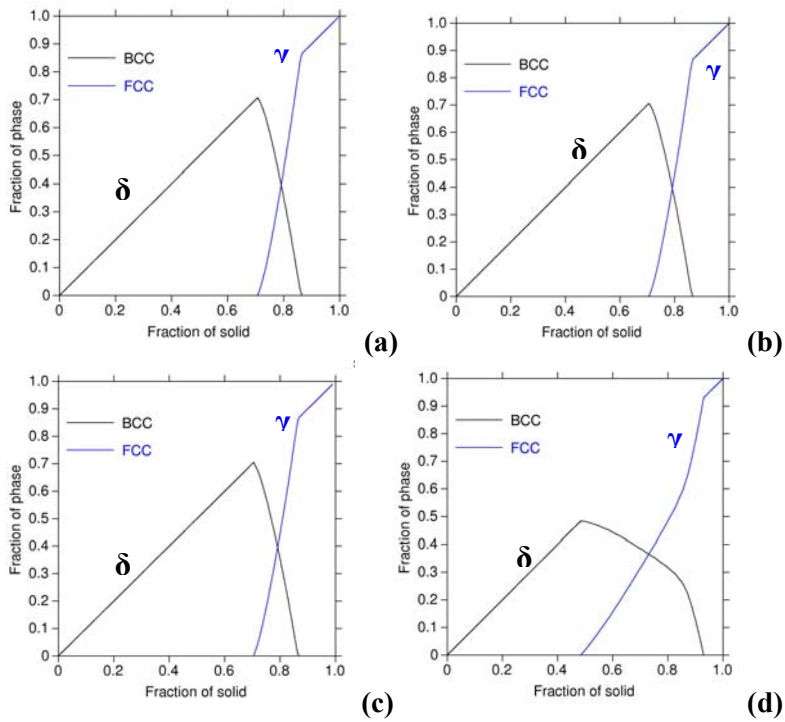

Figure 5. Results from DICTRA showing the formation of phases during solidification at: a) V_C=1.0 m/min, b) V_C=1.75 m/min, c) V_C=5.5 m/min, and d) ΔT/Δt= 11°C/s and λ_2= 200 μm.

In order to determine the actual influence of the casting speed on the local peritectic transition rate, the peritectic transition time was obtained from DICTRA. The peritectic transition time is related to the local solidification time influenced by the local cooling rate within the mushy zone. Figure 6 shows that, as the casting speed is increased, the peritectic transition time is reduced. The peritectic time start and end were estimated at the fractions of solid of f_S=0.7 and f_S=0.86, respectively, for the three casting speeds studied here. On the other hand, the hypothetical case having a larger secondary

dendrite arm spacing, i.e. λ_2= 200 μm, showed a longer peritectic transition period as compared to the case at V_C= 5.5 m/min (see Figure 6).

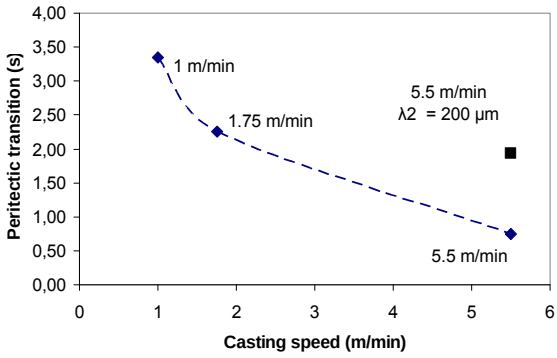

Figure 6. Influence of casting speed on the peritectic transition time.

A larger peritectic transition period may reduce crack propensity by allowing time for stress relief during solidification. The development of local stresses during solidification depends on other variants (such as dendrite structure and material strength) which are not considered in the current study. Nevertheless, this integrated modelling approach can allow us to determine other critical characteristics, such as: the phase transition and the peritectic transition time, by considering the actual influence of the casting conditions on the local solidification. Moreover, the strength and thickness of the solid shell determines in part the castability of steels and strength of the strand. These additional data may assist in further tuning the casting parameters in order to improve the castability of difficult steel grades.

5. Conclusions

The current study shows an integrated modelling approach for determining the influence of casting conditions on the local solidification and peritectic transition in a hyper-peritectic steel. It was found that the casting speeds considered in this study (V_C= 1.0, 1.75 and 5.5 m/min) show little differences on the peritectic transition during solidification (considering the phase transformations as a function of total fraction of solid). On the other hand, the casting speed, which influences the local cooling rate, does have an influence on the peritectic transition time. Increasing casting speed leads to a shorter phase transition period. This could increase the peritectic cracking propensity of the hyper-peritectic steel in the mushy region due to a shorter period of time for allowing stress relief during the local contraction occurring during solidification. By considering the influence of the casting conditions on local solidification, it is possible to acquire additional data that can help in predicting the castability of difficult steel grades.

References

[1] Dippenaar R 2008 Presentation at Corus RD&T.
[2] EGKS Project EU 1989 Project code 7210.CF/801.
[3] EGKS Project EU 2000 Project code 7210.PA/209:1-120.
[4] Howe A A PhD Thesis 1993 The University of Sheffield.
[5] Kerr W, Cisse J, Bolling GF 1974 *Acta Metall.* **22** 677–86
[6] Mizukami H, Yamanaka A, Watanabe T 2002 *ISIJ Int.* **42** 964–73.
[7] Moon S C, Dippenaar R, Lee S H 2012 *IOP Publishing* 012061.
[8] Shibata H, Arai Y, Suzuki M, Emi T 2000 *Metall. Mater. Trans.* B **31** 981–91.
[9] Carless S, Kamperman A, Westendorp A, Brockhoff J. 2011 *Iron & Steel Technology* **8** 84–92.
[10] Howe A, Apel M 2004 Report No: EU Project code GRD1-2000-25447.
[11] Wolf M, Kurz W 1981 *Metall. Trans.* B **12** 85–93.

[12] Meng Y 2004 University of Illinois at Urbana-Champaign.
[13] Thomas B G 2006 Continuous Casting Consortium. Urbana-Champaign,USA: University of Illinois, www.ccc.illinois.edu.
[14] Won Y M, Thoma B G 2001 *Metall. Mater. Trans.* A **32** 1755–1767.

[15] Meng Y A, Thomas B G 2003 *Metall. Mater. Trans.* B **34** 685–705.
[16] Andersson J O, Helander T, Höglund L, Shi P F, Sundman B 2002 *Calphad* **26** 273–312.
[17] Ruiz Mondragon J J, Herrera Trejo M, de Jesus Castro Roman M, Solis T 2008 *ISIJ Int.* **48** 454–60.
[18] Santillana B, van der Knoop W, Hamoen A 2007 Report No.: RSN 134124 Corus RD&T.